Estimation with Ultimate Quantum Precision of the Transverse Displacement between Two Photons via Two-Photon Interference Sampling Measurements

Danilo Triggiani[1,*] and Vincenzo Tamma[1,2,†]

[1]*School of Mathematics and Physics, University of Portsmouth, Portsmouth PO1 3QL, United Kingdom*
[2]*Institute of Cosmology and Gravitation, University of Portsmouth, Portsmouth PO1 3FX, United Kingdom*

(Received 19 September 2023; accepted 8 April 2024; published 30 April 2024)

We present a quantum sensing scheme achieving the ultimate quantum sensitivity in the estimation of the transverse displacement between two photons interfering at a balanced beam splitter, based on transverse-momentum sampling measurements at the output. This scheme can possibly lead to enhanced high-precision nanoscopic techniques, such as superresolved single-molecule localization microscopy with quantum dots, by circumventing the requirements in standard direct imaging of camera resolution at the diffraction limit, and of highly magnifying objectives. Interestingly, we show that our interferometric technique achieves the ultimate spatial precision in nature irrespectively of the overlap of the two displaced photonic wave packets, while its precision is only reduced of a constant factor for photons differing in any nonspatial degrees of freedom. This opens a new research paradigm based on the interface between spatially resolved quantum interference and quantum-enhanced spatial sensitivity.

DOI: 10.1103/PhysRevLett.132.180802

The Hong-Ou-Mandel (HOM) effect [1,2] is an emblematic quantum phenomenon that proved to be instrumental for the development of novel quantum technologies [3]. When two identical photons impinge on the two faces of a balanced beam splitter, and photodetectors are employed at both the outputs, no coincidence detection is recorded, as the two photons always "bunch" in the same output channel. This is caused by the quantum interference occurring between the two possible, but indistinguishable paths undertaken by the two identical photons through the beam splitter. Instead, for nonidentical photons, e.g., in their emission times, polarizations or central frequencies, the coincidence rate changes with the distinguishability between the photons at their detection [1–3]. For this reason, HOM interferometry has been largely employed for high-precision measurements, e.g., of optical lengths and time delays [1,4,5], polarizations [6,7], and for quantum-enhanced imaging techniques, such as quantum optical coherence tomography [8,9]. Furthermore, the analysis of the bounds on the precision achievable in an estimation protocol given by the Cramér-Rao bound (CRB) [10,11], and of the ultimate precision achievable in nature through the quantum Cramér-Rao bound (QCRB) [12,13], has become a useful tool to determine the sensitivity of two-photon interferometry techniques for metrological applications [4,14–16].

Interestingly, it has been recently shown that inner variables resolved two-photon interference, in which two delayed or frequency-shifted photons impinging on the two faces of the beam splitter are detected by frequency- or time-resolving detectors, respectively, circumvents the requirement of large overlap in the photonic wave packets typical of HOM interferometry [17–25]. Indeed, this technique allows us to observe beating, i.e. oscillations, in probabilities of coincidence and bunching of the two photons, with a period that is inversely proportional to the difference in the colors or in the incidence times at the beam splitter, hence preserving its sensitivity also in the case of nonoverlapping wave packets [22].

Two-photon interference has also been performed in the spatial domain, i.e., while varying transversal properties of the two photonic wave packets, for example, slightly rotating the momentum of the photons before they interfere [26,27], manipulating the spatial overlap between the photons [28], or simultaneously introducing a temporal delay to observe spatiotemporal coherence properties of the two-photon state [28,29]. Spatial HOM interferometry so far has mostly been employed to assess the spatial coherence of highly entangled photons, e.g., produced by spontaneous parametric down-conversion. However, to the best of our knowledge, the metrological potential of spatial two-photon interference for high precision imaging and sensing applications has not been investigated yet. A study in this direction is made even more compelling, from an experimental and technological point of view, due to the recent development of high-precision nanoscopic techniques that already employ single-photon emitters and single-photon cameras [30–32].

This Letter introduces a quantum interference technique based on spatially resolved sampling measurements and investigates its properties from the metrological point of view. We show that resolving and sampling over the difference in transverse momenta of two photons detected after they interfere at a beam splitter is an optimal metrological scheme for the estimation of the transverse separation of their wave packets, achieving the ultimate precision given by the QCRB. This can be done by employing two cameras that spatially sample over all the possible two-photon interference events in the far field, resolving the difference in the transverse momenta of the two detected photons, and simultaneously recording whether the two photons ended up in the same or different output channels of the beam splitter (see Fig. 1). This can therefore be seen as an interesting metrological application for spatial estimation of multiboson correlation sampling based on inner-variable sampling measurements [33–35]. In particular, we show that, apart from a constant non-vanishing factor, the sensitivity of the proposed technique is retained for photons that also differ in any physical property other than their transverse position, e.g., their polarization or frequency, useful for localization and tracking applications with independent emitters. Furthermore, the precision of this scheme can be, in principle, increased arbitrarily, for any fixed displacement between the photons, by employing photons with broader and broader transverse-momentum distributions. Since our technique does not involve a direct detection of the single photons in the position domain, it removes the need of high-resolution cameras and highly magnifying objectives, typically employed in current localization microscopy techniques, which require us to directly resolve sources at the diffraction limit [36,37]. Moreover, for almost identical photons, the resolving cameras can be replaced with bucket detectors that only count coincidences and bunching events, without affecting the sensitivity of the scheme. Other than single molecule localization nanoscopy, this technique finds possible applications in astrophysical bodies localization, or for the measurement of any transverse displacement of a probe single-photon beam with respect to a reference beam, e.g., caused by refraction or by optical devices such as tunable beam displacers [38].

Experimental setup.—We consider pairs of quasimonochromatic photons, with wave number k_0, produced by two independent sources impinging on the two faces of a balanced beam splitter, and then detected by two cameras positioned at the beam-splitter outputs in the far-field regime at a distance d from their sources. For simplicity, we will only describe one transverse dimension of the setup, but the same analysis can be easily generalized to the two-dimensional case. We suppose that the transverse position of the Sth photon is described by a wave packet $\psi_S(x) = \psi(x - x_{0S})$ centered around the position x_{0S}, with $S = 1, 2$. A practical example of such a setup is shown in the schematic representation of Fig. 1. We can thus write the two-photon state as

$$|\Psi\rangle = \int \mathrm{d}x_1 \psi_1(x_1) \hat{a}_1^\dagger(x_1)|0\rangle_1 \otimes \int \mathrm{d}x_2 \psi_2(x_2) \hat{b}_2^\dagger(x_2)|0\rangle_2, \quad (1)$$

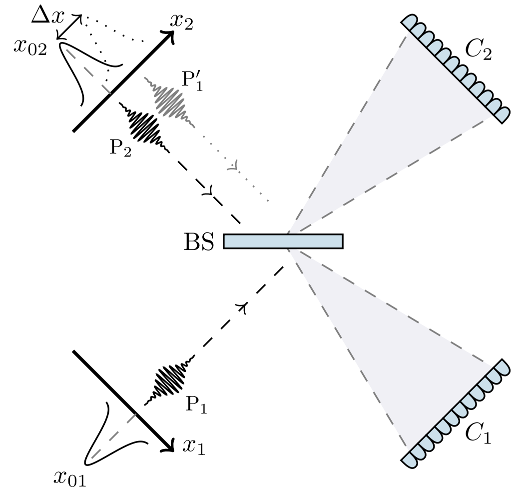

FIG. 1. Two single photons, centered in positions x_{01} and x_{02} in their respective transverse planes, impinge onto the two faces of a balanced beam splitter (BS), so that the displacement between the probe photon P_2 and the symmetric image P_1' of the reference photon P_1 is $\Delta x = x_{01} - x_{02}$. The two photons are then detected by two cameras (C_1 and C_2) in the far-field regime, which resolve their transverse momenta k and k' for joint detections either in the same (bunching events) or opposite (coincidence events) output channels of the beam splitter.

where $\hat{a}_1^\dagger(x_1)$ and $\hat{b}_2^\dagger(x_2)$ are the bosonic creation operators associated with the first and second input mode of the beam splitter at transverse positions x_1 and x_2, respectively, satisfying the commutation relation $[\hat{a}_S(x), \hat{b}_{S'}^\dagger(x')] = \sqrt{\nu}\delta_{SS'}\delta(x - x')$, with $S, S' = 1, 2$, where $\delta_{SS'}$ and $\delta(x-x')$ denote the Kronecker and Dirac delta, respectively, while $0 \leqslant \nu \leqslant 1$ represents a degree of indistinguishability between the photons in any physical property other than their transverse positions (e.g., different polarizations), with $\nu = 1$ denoting the maximum degree of indistinguishability. The displacement $\Delta x = x_{01} - x_{02}$ that we aim to measure can be caused by refraction or any other beam-displacing optical device [38], or it can represent the position of a single-photon source that we want to localize, e.g., a probe quantum dot attached to a molecule [30–32], with respect to an identical reference photon emitted at a known position.

After impinging on the beam splitter, each pair of photons is randomly detected at the pixels in positions y and y' either of a single camera or distinct cameras. Since the detection occurs in the far-field regime, it corresponds to resolving the transverse momenta $k = yk_0/d$ and $k' = y'k_0/d$ of the two photons, i.e., the conjugate variables to the photon transverse positions. We show that this results in the observation of quantum beats in the difference $\Delta k = k - k'$ (see Fig. 2) with periodicity inversely proportional to $\Delta x = x_{01} - x_{02}$ in the joint probabilities

$$P_\nu(\Delta k, X) = \frac{1}{2} C(\Delta k)(1 + \alpha(X)\nu \cos(\Delta k \Delta x)), \quad (2)$$

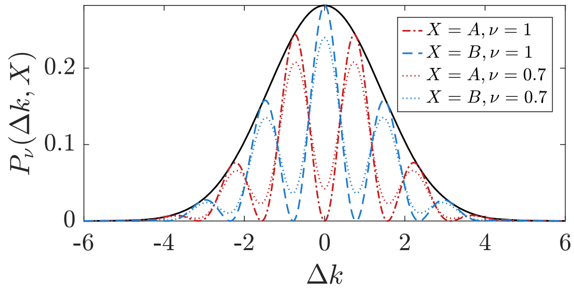

FIG. 2. Plots of the probability $P_\nu(\Delta k, X)$ in Eq. (2) for Gaussian transverse-momentum distributions $|\varphi(k)|^2$, yielding a Gaussian envelope $C(\Delta x)$ (black solid line), for the same-camera ($X = B$) detection events, and the different-camera ($X = A$) detection events. The variance of the distribution $|\varphi(k)|^2$ is set to $\sigma_k^2 = 1$, which fixes a natural scale for Δk and for the separation $\Delta x = 4/\sigma_k$.

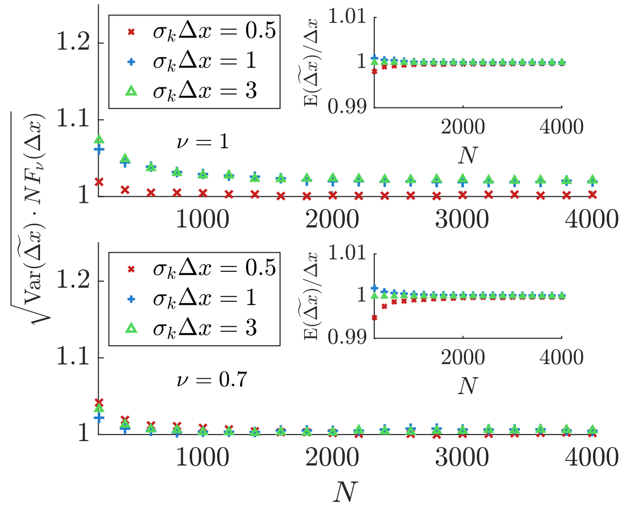

FIG. 3. Numerical simulations for Gaussian photonic wave packets and for different values of $\sigma_k \Delta x$ of the variance $\mathrm{Var}(\widetilde{\Delta x})$ of the maximum likelihood estimator $\widetilde{\Delta x}$, which saturates the CRB in Eq. (4) for the FI $F_\nu(\Delta x)$ in Eq. (7) at the increasing of the number N of sampling measurement iterations of the estimation. In the inset, we plot the ratio between the expected value $E(\widetilde{\Delta x})$ of the maximum-likelihood estimator and the true value Δx.

of the two photons detected by different cameras ($X = A$), or the same camera ($X = B$), where $\alpha(A) = -1$ and $\alpha(B) = +1$, and $C(\Delta k)$ is the beats envelope, whose shape is known and depends on the transverse-momentum distribution of the photons, i.e., the modulo squared $|\varphi(k)|^2$ of the Fourier transform of $\psi(x)$, e.g., $C(\Delta k) = \exp(-\Delta k^2/4\sigma_k^2)/\sqrt{4\pi\sigma_k^2}$ for Gaussian wave packets [39].

The estimation of the displacement Δx is carried out by performing a given number N of sampling measurements of the values $(\Delta k, X)$ with pixel size δy, corresponding to a precision $\delta k = \delta y k_0/d$ in the transverse momenta, small enough to resolve the transverse-momentum distributions of the two photons and the beating oscillations with period $2\pi/\Delta x$ in Eq. (2), i.e.,

$$\delta y \ll \frac{d}{k_0}\sigma_k, \qquad \delta y \ll \frac{d}{k_0}\frac{1}{\Delta x}, \tag{3}$$

where σ_k^2 is the variance of the transverse-momentum distribution of the photons. The N detected sampling outcomes $(\Delta k_i, X_i)$ with $i = 1, \ldots, N$ are then employed in a standard maximum-likelihood estimation procedure of the parameter Δx, specialized to the probability distribution in Eq. (2) [39].

Because of the Fourier uncertainty principle $\sigma_k \geqslant 1/2\sigma_x$, with σ_x given by the standard deviation of $|\psi(x)|^2$ and which, for diffraction limited optics, can be approximated by $\sigma_x \simeq 2\pi/2.8k_0 \simeq 2.2/k_0$, it is possible to express the first resolution requirement in Eq. (3) as $\delta y \ll 0.22d$, easily satisfied with current cameras, independently of the color of the photons. Furthermore, since this technique requires cameras only able to resolve oscillations of period $\propto 1/\Delta x$, it circumvents the need to employ objectives with high magnifying factors to resolve directly the relative position Δx of the single-photon emitters at the diffraction limit, typically required in imaging techniques such as single-molecule localization microscopy [36,37].

Ultimate quantum sensitivity.—Any unbiased estimator $\widetilde{\Delta x}$ associated with the estimation of the separation Δx between the photon pair in Eq. (1), will have a variance $\mathrm{Var}[\widetilde{\Delta x}]$ bounded from below by the CRB associated with the described measurement [10,11], and ultimately by the QCRB, which sets the ultimate quantum limit of the achievable precision independently of the measurements [12,13,41,42], i.e.,

$$\mathrm{Var}[\widetilde{\Delta x}] \geqslant \frac{1}{NF_\nu(\Delta x)} \geqslant \frac{1}{NH(\Delta x)}, \tag{4}$$

where $H(\Delta x)$ is the quantum Fisher information (QFI), $F_\nu(\Delta x)$ the Fisher information (FI), and N is the number of independent sampling measurements [10,12]. In particular, we demonstrate from Eq. (2) that in our scheme, in case of photons differing only in their transverse positions,

$$F_{\nu=1}(\Delta x) = H(\Delta x) \equiv H \equiv 2\sigma_k^2, \tag{5}$$

i.e., the FI saturates the QFI [39]. We show in Fig. 3 that the QCRB in Eq. (4) is already approximately saturated for N of the order of 1000 by maximizing the measured likelihood function, calculated in the Supplemental Material, i.e.,

$$\mathrm{Var}[\widetilde{\Delta x}] \simeq \frac{1}{NH} = \frac{1}{2N\sigma_k^2}. \tag{6}$$

Remarkably, the ultimate precision in Eq. (6) achieved with our technique is independent of the separation Δx to be estimated, and can be, in principle, arbitrarily improved by increasing the transverse-momentum variance σ_k^2 of the photons. For example, assuming Gaussian distributions $|\psi(x)|^2$ with a diffraction limited width $\sigma_x \simeq 100$ nm [37], the bound on the sensitivity in Eq. (6) amounts to $\sqrt{1/(2N\sigma_k^2)} \simeq 2.6$ nm employing only $N \simeq 3000$ pairs of photons. This would not be possible in direct imaging without the use of magnifying objectives, where even by employing a camera with ~10 μm pixel size, 100× magnifying lenses would be required to reach the diffraction limit. Localizing single-photon wave packets with smaller and smaller diffraction limited widths becomes increasingly prohibitive for direct imaging techniques, due to the need of lenses with higher and higher magnification factors and the detrimental effects of misalignments and aberrations [43], while, in our technique, not only it is feasible, but also allows according to Eq. (6) higher and higher precisions, useful, for example, for studies of structures and functions at the subcellular level [44]. Furthermore, already for $N \simeq 3000$ sampling iterations, we achieve a 97% saturation of the CRB, and a relative bias smaller than 0.1%, without the need of fully retrieving the output probability distribution with a larger number of measurements (see Fig. 3).

Interestingly, this interferometric technique is completely unaffected by the lack of overlap between the spatial wave packets of the two photons. Indeed, performing transverse-momentum resolving detections, i.e., resolving the variables in the conjugate domain to the position, renders the detectors "blind" to the position of emission of the two photons, and thus it enables the observation of two-photon quantum interference. This feature is in stark contrast with standard non-resolving two-photon interference, where the distinguishability of photons with spatially nonoverlapping wave packets is not erased at the detectors, hindering the precision of the estimation. Nevertheless, for photons with mostly overlapping spatial wave packets, i.e., for $\sigma_k \Delta x \ll 1$, we show in the Supplemental Material that it is possible to saturate the QFI without resolving their transverse momenta and therefore by using simple bucket detectors.

FI for partially distinguishable detected photons.—Our technique remains effective also when introducing partial distinguishability $\eta < 1$ in the two-photon detection. Indeed, in this more general scenario, we show, by using Eq. (2), that the FI, normalized to the QFI H in Eq. (5), reads [39]

$$\frac{F_\nu(\Delta x)}{H} = \int \mathrm{d}\Delta k \, f_\nu(\Delta k; \Delta x), \tag{7}$$

where

$$f_\nu(\Delta k; \Delta x) = C(\Delta k) \frac{\Delta k^2}{2\sigma_k^2} \frac{\nu^2 \sin^2(\Delta k \Delta x)}{1 - \nu^2 \cos^2(\Delta k \Delta x)}. \tag{8}$$

As evident in Fig. 3, also for $\nu < 1$, the CRB is approximately saturated already with N of the order of 1000, i.e., $\mathrm{Var}[\widetilde{\Delta x}] \simeq 1/NF_\nu(\Delta x)$. Importantly, from the plot of $F_\nu(\Delta x)$ in Fig. 4, it is evident that, for $\sigma_k \Delta x \gtrsim 0.5$, a condition that can always be guaranteed by calibrating the position of the reference photon, for Gaussian wave packets

$$F_\nu(\Delta x) \gtrsim (1 - \sqrt{1 - \nu^2}) H, \tag{9}$$

independently of the value of Δx (e.g., with $1 - \sqrt{1 - \nu^2} \simeq 0.6$ for $\nu = 0.9$), where $(1 - \sqrt{1 - \nu^2})H$ is the asymptotic value for $\sigma_k \Delta x \gg 1$ [39].

Contribution from the sampled transverse momenta.—Each term $f_\nu(\Delta k; \Delta x)$ in Eq. (8) represents, apart from a factor $2\sigma_k^2$, the contribution to $F_\nu(\Delta x)$ in Eq. (7) yielded by both outcomes $(\Delta k, A)$ and $(\Delta k, B)$ of a single two-photon detection. The expression of $f_\nu(\Delta k; \Delta x)$ in Eq. (8) allows us to understand which outcome values of Δk yield more information on the separation Δx, and, conversely, which ones can be discarded with a negligible loss of precision. Indeed, we notice from Fig. 4(b) that $f_\nu(\Delta k; \Delta x)$, as a function of Δk, is concentrated within its envelope $\nu^2 C(\Delta k) \Delta k^2 / 2\sigma_k^2$, associated with the distributions of the photons in the transverse momenta, independently of Δx. Therefore, the cameras do not need to be adjusted according to the unknown separation Δx between the two photons. Furthermore, if the tails of the distribution of the photons have a negligible contribution (e.g., for Gaussian wave packets), one can integrate the $f_\nu(\Delta k; \Delta x)$ in Eq. (8)

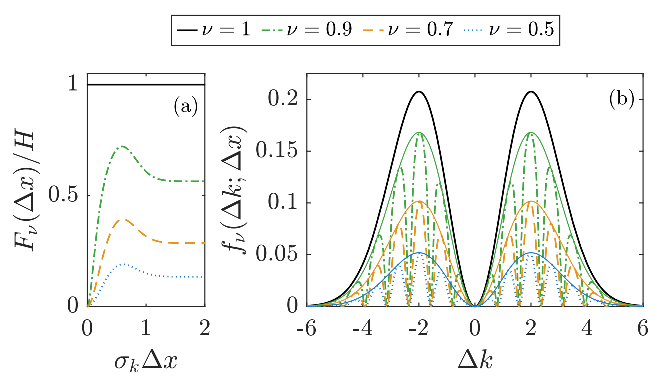

FIG. 4. Plots for Gaussian transverse-momentum distributions $|\varphi(k)|^2$ and different values of ν of (a) $F_\nu(\Delta x)$ normalized to H in Eq. (7), with Eq. (9) holding independently of the value of Δx, for $\sigma_k \Delta x \gtrsim 0.5$; (b) Contributions $f_\nu(\Delta k; \Delta x)$ in Eq. (8) to the FI depending on the outcome value Δk for $\Delta x = 4/\sigma_k$, with $\sigma_k = 1$, which fixes a natural scale for Δk. All the information on Δx can be obtained by sampling measurements in the transverse momenta difference Δk within its envelopes independently of the value of Δx (thin solid lines).

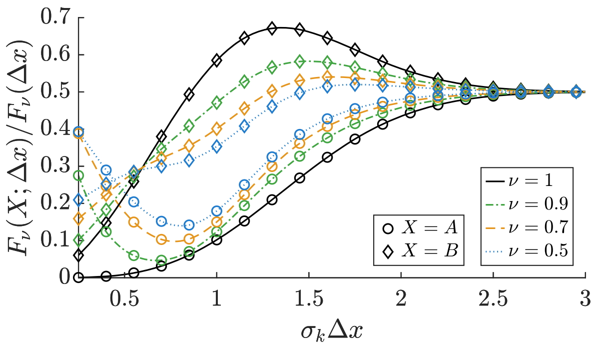

FIG. 5. Plot of the ratios $F_\nu(X;\Delta x)/F_\nu(\Delta x)$ between the FI associated with the observation of only two-camera ($X = B$), or only single-camera events ($X = A$), and the FI in Eq. (7) of our original scheme, for different values of ν. Observing only single-camera events yields a better precision than double-camera events for $\sigma_k \Delta x \gtrsim 0.5$.

within a few units of σ_k, hence with a reduced camera sensing range.

Contribution from single or joint camera detections.—In Fig. 5 we show, for different values of ν, the FI $F_\nu(X;\Delta x)$ associated with the observation of only two-camera ($X = A$) events or single-camera ($X = B$) events, according to the probability distributions $P_\nu(\Delta k, X)$ in Eq. (2), normalized over the overall probability $\int \mathrm{d}\Delta k\, P_\nu(\Delta k, X)$ [39]. For $\sigma_k \Delta x \gtrsim 0.5$ and Gaussian photonic wave packets, we see from Fig. 5 that observing only one-camera events ($X = B$) is more informative than observing only two-camera events ($X = A$), since $F_\nu(B;\Delta x) \geqslant F_\nu(A;\Delta x)$, and $F_\nu(B;\Delta x)$ is only reduced, compared to $F_\nu(\Delta x)$, by a nonvanishing factor $R_\nu = F_\nu(B;\Delta x)/F_\nu(\Delta x)$ (e.g., $R_\nu \simeq 0.6$ for $\nu = 0.9$ and $R_\nu \simeq 0.7$ for $\nu = 1$, for $\sigma_k \Delta x \simeq 1.5$). Therefore, by using Eq. (9), we deduce that our scheme can also be employed with only one camera, achieving a FI $\gtrsim H R_\nu (1 - \sqrt{1 - \nu^2})/2$, where the factor $1/2$ provides for the fact that we are observing only one output channel of the beam splitter.

Conclusions.—We presented a spatial quantum interference technique allowing the estimation of the transverse separation of two single-photon beams at the ultimate precision allowed by the QCRB, based on transverse-momentum resolved sampling measurements. In the regime of almost identical photons, the two cameras can be replaced with nonresolving bucket detectors without any loss of sensitivity. Furthermore, apart from a nonvanishing factor, the same quantum sensitivity is retained also for photons partially differing in any physical parameters other than their transverse position, and it can be also achieved by employing only one camera at a single output of the beam splitter. Finally, such an ultimate quantum sensitivity can be approximately obtained for a limited number of iterations of the experiment, and be, in principle, arbitrarily increased by employing photons with more broadly distributed transverse momenta. This means that such a precision is only limited by the highest value of the transverse-momentum distribution variance experimentally feasible with current technologies. Moreover, by using indirect sampling measurements which resolve the photonic transverse momenta instead of the positions directly, this technique removes the requirement of camera resolution at the diffraction limit typical of direct imaging techniques, as well as highly magnifying objectives.

These results shed new light on the metrological power of two-photon spatial interference and can pave the way to new high-precision sensing techniques. This work has the potential to enhance superresolution imaging techniques that already employ single-photon sources as probes for the localization and tracking of biological samples, such as single-molecule localization microscopy with quantum dots [30–32]. Other possible applications can be found in the development of quantum sensing techniques for high-precision refractometry and astrophysical bodies localization, as well as high-precision multiparameter sensing schemes, including 3D quantum localization methods, and simultaneous estimation of the color and position of single-photon emitters, by combining our technique with multiphoton interference techniques in the frequency-time domain [4,22].

V. T. acknowledges support from the Air Force Office of Scientific Research under Award No. FA8655-23-1-7046.

[*]danilo.triggiani@port.ac.uk
[†]vincenzo.tamma@port.ac.uk

[1] C. K. Hong, Z. Y. Ou, and L. Mandel, Measurement of subpicosecond time intervals between two photons by interference, Phys. Rev. Lett. **59**, 2044 (1987).

[2] Y. H. Shih and C. O. Alley, New type of Einstein-Podolsky-Rosen-Bohm experiment using pairs of light quanta produced by optical parametric down conversion, Phys. Rev. Lett. **61**, 2921 (1988).

[3] Frédéric Bouchard, Alicia Sit, Yingwen Zhang, Robert Fickler, Filippo M Miatto, Yuan Yao, Fabio Sciarrino, and Ebrahim Karimi, Two-photon interference: The Hong-Ou-Mandel effect, Rep. Prog. Phys. **84**, 012402 (2021).

[4] Ashley Lyons, George C. Knee, Eliot Bolduc, Thomas Roger, Jonathan Leach, Erik M. Gauger, and Daniele Faccio, Attosecond-resolution Hong-Ou-Mandel interferometry, Sci. Adv. **4**, eaap9416 (2018).

[5] Yuanyuan Chen, Matthias Fink, Fabian Steinlechner, Juan P. Torres, and Rupert Ursin, Hong-Ou-Mandel interferometry on a biphoton beat note, npj Quantum Inf. **5**, 43 (2019).

[6] Natapon Harnchaiwat, Feng Zhu, Niclas Westerberg, Erik Gauger, and Jonathan Leach, Tracking the polarisation state of light via Hong-Ou-Mandel interferometry, Opt. Express **28**, 2210 (2020).

[7] Fabrizio Sgobba, Deborah Katia Pallotti, Arianna Elefante, Stefano Dello Russo, Daniele Dequal, Mario Siciliani de Cumis, and Luigi Santamaria Amato, Optimal measurement

of telecom wavelength single photon polarisation via Hong-Ou-Mandel interferometry, Photonics **10**, 72 (2023).

[8] Ayman F. Abouraddy, Magued B. Nasr, Bahaa E. A. Saleh, Alexander V. Sergienko, and Malvin C. Teich, Quantum-optical coherence tomography with dispersion cancellation, Phys. Rev. A **65**, 053817 (2002).

[9] Magued B. Nasr, Darryl P. Goode, Nam Nguyen, Guoxin Rong, Linglu Yang, Björn M. Reinhard, Bahaa E. A. Saleh, and Malvin C. Teich, Quantum optical coherence tomography of a biological sample, Opt. Commun. **282**, 1154 (2009).

[10] Harald Cramér, *Mathematical Methods of Statistics* (Princeton University Press, Princeton, NJ, 1999), Vol. 9.

[11] Vijay K. Rohatgi and A. K. Md Ehsanes Saleh, *An Introduction to Probability and Statistics* (John Wiley & Sons, New York, 2000).

[12] Carl W. Helstrom, Quantum detection and estimation theory, J. Stat. Phys. **1**, 231 (1969).

[13] A. S. Holevo, *Probabilistic and Statistical Aspects of Quantum Theory*, Publications of the Scuola Normale Superiore (Scuola Normale Superiore, Pisa, 2011).

[14] Hamish Scott, Dominic Branford, Niclas Westerberg, Jonathan Leach, and Erik M. Gauger, Beyond coincidence in Hong-Ou-Mandel interferometry, Phys. Rev. A **102**, 033714 (2020).

[15] N. Fabre and S. Felicetti, Parameter estimation of time and frequency shifts with generalized Hong-Ou-Mandel interferometry, Phys. Rev. A **104**, 022208 (2021).

[16] Spencer J. Johnson, Colin P. Lualdi, Andrew P. Conrad, Nathan T. Arnold, Michael Vayninger, and Paul G. Kwiat, Toward vibration measurement via frequency-entangled two-photon interferometry, in *Quantum Sensing, Imaging, and Precision Metrology*,(SPIE, 2023), Vol. 12447, p. 124471C, 10.1117/12.2650820.

[17] T. Legero, T. Wilk, A. Kuhn, and G. Rempe, Time-resolved two-photon quantum interference, Appl. Phys. B **77**, 797 (2003).

[18] Thomas Legero, Tatjana Wilk, Markus Hennrich, Gerhard Rempe, and Axel Kuhn, Quantum beat of two single photons, Phys. Rev. Lett. **93**, 070503 (2004).

[19] Vincenzo Tamma and Simon Laibacher, Multiboson correlation interferometry with arbitrary single-photon pure states, Phys. Rev. Lett. **114**, 243601 (2015).

[20] Rui-Bo Jin, Thomas Gerrits, Mikio Fujiwara, Ryota Wakabayashi, Taro Yamashita, Shigehito Miki, Hirotaka Terai, Ryosuke Shimizu, Masahiro Takeoka, and Masahide Sasaki, Spectrally resolved Hong-Ou-Mandel interference between independent photon sources, Opt. Express **23**, 28836 (2015).

[21] Pablo Yepiz-Graciano, Alí Michel Angulo Martínez, Dorilian Lopez-Mago, Hector Cruz-Ramirez, and Alfred B. U'Ren, Spectrally resolved Hong-Ou-Mandel interferometry for quantum-optical coherence tomography, Photon. Res. **8**, 1023 (2020).

[22] Danilo Triggiani, Giorgos Psaroudis, and Vincenzo Tamma, Ultimate quantum sensitivity in the estimation of the delay between two interfering photons through frequency-resolving sampling, Phys. Rev. Appl. **19**, 044068 (2023).

[23] Xu-Jie Wang, Bo Jing, Peng-Fei Sun, Chao-Wei Yang, Yong Yu, Vincenzo Tamma, Xiao-Hui Bao, and Jian-Wei Pan, Experimental time-resolved interference with multiple photons of different colors, Phys. Rev. Lett. **121**, 080501 (2018).

[24] T. Hiemstra, T. F. Parker, P. Humphreys, J. Tiedau, M. Beck, M. Karpiński, B. J. Smith, A. Eckstein, W. S. Kolthammer, and I. A. Walmsley, Pure single photons from scalable frequency multiplexing, Phys. Rev. Appl. **14**, 014052 (2020).

[25] Vindhiya Prakash, Aleksandra Sierant, and Morgan W. Mitchell, Autoheterodyne characterization of narrow-band photon pairs, Phys. Rev. Lett. **127**, 043601 (2021).

[26] Z. Y. Ou and L. Mandel, Further evidence of nonclassical behavior in optical interference, Phys. Rev. Lett. **62**, 2941 (1989).

[27] Heonoh Kim, Osung Kwon, Wonsik Kim, and Taesoo Kim, Spatial two-photon interference in a Hong-Ou-Mandel interferometer, Phys. Rev. A **73**, 023820 (2006).

[28] P. S. K. Lee and M. P. van Exter, Spatial labeling in a two-photon interferometer, Phys. Rev. A **73**, 063827 (2006).

[29] Fabrice Devaux, Alexis Mosset, Paul-Antoine Moreau, and Eric Lantz, Imaging spatiotemporal Hong-Ou-Mandel interference of biphoton states of extremely high Schmidt number, Phys. Rev. X **10**, 031031 (2020).

[30] Janina Hanne, Henning J. Falk, Frederik Görlitz, Patrick Hoyer, Johann Engelhardt, Steffen J. Sahl, and Stefan W. Hell, Sted nanoscopy with fluorescent quantum dots, Nat. Commun. **6**, 7127 (2015).

[31] Claudio Bruschini, Harald Homulle, Ivan Michel Antolovic, Samuel Burri, and Edoardo Charbon, Single-photon avalanche diode imagers in biophotonics: Review and outlook, Light **8**, 87 (2019).

[32] Jennifer M. Urban, Wesley Chiang, Jennetta W. Hammond, Nicole M. B. Cogan, Angela Litzburg, Rebeckah Burke, Harry A. Stern, Harris A. Gelbard, Bradley L. Nilsson, and Todd D. Krauss, Quantum dots for improved single-molecule localization microscopy, J. Phys. Chem. B **125**, 2566 (2021).

[33] Simon Laibacher and Vincenzo Tamma, From the physics to the computational complexity of multiboson correlation interference, Phys. Rev. Lett. **115**, 243605 (2015).

[34] Vincenzo Tamma and Simon Laibacher, Multi-boson correlation sampling, Quantum Inf. Process. **15**, 1241 (2016).

[35] Vincenzo Tamma and Simon Laibacher, Scattershot multiboson correlation sampling with random photonic inner-mode multiplexing, Eur. Phys. J. Plus **138**, 335 (2023).

[36] Raimund J. Ober, Sripad Ram, and E. Sally Ward, Localization accuracy in single-molecule microscopy, Biophys. J. **86**, 1185 (2004).

[37] Mickaël Lelek, Melina T. Gyparaki, Gerti Beliu, Florian Schueder, Juliette Griffié, Suliana Manley, Ralf Jungmann, Markus Sauer, Melike Lakadamyali, and Christophe Zimmer, Single-molecule localization microscopy, Nat. Rev. Methods Primers **1**, 39 (2021).

[38] Luis José Salazar-Serrano, Alejandra Valencia, and Juan P. Torres, Tunable beam displacer, Rev. Sci. Instrum. **86**, 033109 (2015).

[39] See Supplemental Material at http://link.aps.org/supplemental/10.1103/PhysRevLett.132.180802 (which includes [40]) for the derivations of Eqs. (2), (5), (7) and (8), the maximum likelihood function, and the FI for $\sigma_k \Delta x \gg 1$, for nonresolved measurements, and for the observation of only single-camera or two-camera events.

[40] Roy J. Glauber, The quantum theory of optical coherence, Phys. Rev. **130**, 2529–2539 (1963).

[41] Matteo G. A. Paris, Quantum estimation for quantum technology, Int. J. Quantum. Inform. **07**, 125 (2009).

[42] Jing Liu, Haidong Yuan, Xiao-Ming Lu, and Xiaoguang Wang, Quantum Fisher information matrix and multiparameter estimation, J. Phys. A **53**, 023001 (2019).

[43] Ismail M. Khater, Ivan Robert Nabi, and Ghassan Hamarneh, A review of super-resolution single-molecule localization microscopy cluster analysis and quantification methods, Patterns **1**, 100038 (2020).

[44] Steffen J. Sahl, Stefan W. Hell, and Stefan Jakobs, Fluorescence nanoscopy in cell biology, Nat. Rev. Mol. Cell Biol. **18**, 685 (2017).